Article citation info:
Chojnowski J. Analysis of the influence of substitute fuels on properties operating conditions of military hybrid drive system. Combustion Engines.2024;197(2):22-31. https:/doi.org/10.19206/CE-174553

Janusz CHOJNOWSKI

Combustion Engines
Polish Scientific Society of Combustion Engines

Analysis of the influence of substitute fuels on properties operating conditions of military hybrid drive systems

ARTICLE INFO

Received: 12 May 2023
Revised: 24 October 2023
Accepted: 26 October 2023
Available online: 10 January 2024

Despite the undoubted advantages of electric drives, the mass and volume energy density of chemical batteries makes it difficult to rely solely on cheap and green electricity in many applications such as airplanes, long-distance trains, ocean-going vessels and heavy equipment. The answer combining the advantages of EV and ICE are hybrid drives. Hybrid electric drives have also found their use in military applications thanks to, among others, the quiet operation of the system in EV mode, which may be a key advantage in some combat applications, e.g. urban areas. The range of a small hybrid vehicle extended by the use of ICE increases its operational capabilities. Hybrid systems can also use alternative hydrocarbon fuels. The aim of the work was to determine the impact of alternative fuels, potentially the most available on the modern battlefield, on the performance of the hybrid drive system of a wheeled military platform intended for operation in urban areas. The experiment showed that alternative fuels such as F-34 and Jet A-1 are compatible, but may result in increased fuel consumption, reduced energy efficiency and negative environmental impact due to higher exhaust emissions.

Key words: *hybrid drive, alternative fuels, F34, Jet A-1, military vehicle propulsion*

1. Introduction

The modern development of hybrid drive systems takes into account the need to combine conflicting requirements. On the one hand, ecological and economical requirements are growing. On the other hand, these systems are required to achieve maximum work units, long range and light-weight construction [23]. The continuous development of hybrid systems increases the complexity of their construction [16]. The internal combustion engines themselves also use very precise power and control systems to increase thermal efficiency [20]. Precision fuel systems are very sensitive to changes in fuel parameters or contamination. Modern multi-element hybrid systems, in which various forms of energy are transformed several times, are therefore very susceptible to the influence of fuel on the quality of their work [6, 9]. In connection with the above, checking the impact of the use of alternative fuels in the hybrid (electric-combustion) drive system on the operational properties of the vehicle seems to be a necessary path to check [4]. In the context of military vehicles, this task is additionally noteworthy due to the possibilities of using fuels available on the battlefield. All the possibilities of the so-called flex fuel are welcome in military applications, and the ability to use different types of fuel on the battlefield can be worth as much as a human life [13]. The article analyzes the impact of the use of 3 types of fuels that may be available during warfare in compression-ignition engines that are the "combustion part" of the hybrid propulsion system in the Light Unmanned Military Wheeled Platform (LUMWP) constructed at Military University of Technology in Warsaw as shown on Fig. 1.

The LUMWP is equipped with a series hybrid powertrain system. Figure 2 below presents a schematic diagram of a series hybrid electric-combustion drive.

Fig. 1. An isometric view of Light Unmanned Military Wheeled Platform

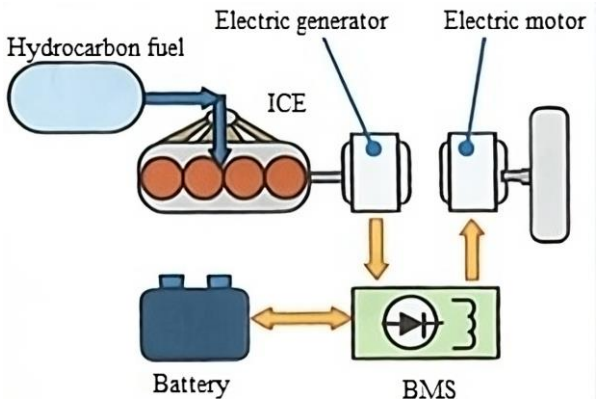

Fig. 2. Diagram of a series hybrid electric-combustion drive (based on 9)

The vehicle has electric motors built into drive modules with reducers powered by a battery charged by an electric current generator. Thus, the most important properties of electric motors are used (maximum torque at low speed, quiet operation, and the possibility of overloading), as well as the extended range of the vehicle, thanks to the possibility of recharging the battery with a combustion generator. In addition, the electric motor can work as a generator during braking, which allows for energy recovery and lower fuel consumption [16, 21]. The system with electric motors directly driving the wheels of the vehicle does not require mechanical power transmission systems (gearboxes and shafts), which allows for the reduction of the weight and size of such drive systems. Figure 3 shows a block diagram of the vehicle drive system.

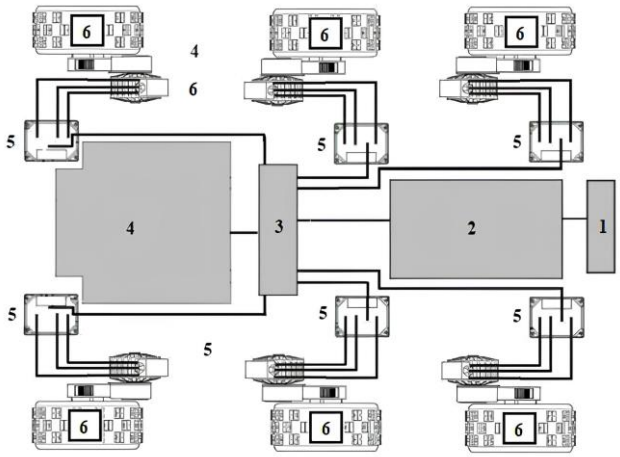

Fig. 3. Diagram of the LUMWP drive system: 1) control system, 2) electric current ICE generator, 3) distribution box, 4) battery, 5) inverters, 6) electric motors with gears and wheels [author's source]

In the further part of the article, the fuels selected for comparison, technical details of the tested propulsion system, research methods, results, and a summary with conclusions will be discussed.

2. Materials and methods

2.1. Fuels selected for comparison

The fuels selected for comparison are the crude oil fraction boiling during the refining process at a temperature of 180–350°C [19]. These are fuels widely available on any potential battlefield. F34 is a universal general-purpose fuel in NATO structures [18]. Jet A-1 is the most popular aviation fuel in the world [12]. Diesel fuel is the most popular hydrocarbon fuel in the world (dedicated to the discussed engine) [10]. Each of the fuels came from one batch and had normative parameters (important for the operation of diesel engines), which are listed in Table 1.

In general, each type of fuel has its own unique properties and is suitable for specific applications [10]. The choice of fuel depends on factors such as engine type, mode of transport, and desired performance. Analysis of the parameters of the above fuels shows a great similarity between Jet A-1 and F-34 this is also indicated in the literature [6, 10]. Replacing a compression ignition (CI) engine with diesel fuel, one should take into account the occurrence of the following problems:

– lower density, viscosity, and calorific value in relation to diesel fuel may reduce the value of the maximum useful parameters of the engine [6, 10]
– a lower cetane number may impair cold starting and increase the tendency to hard work [10, 19].

The criterion for selecting these specific fuels for testing was their potential availability in combat conditions.

Table 1. Selected normative parameters of diesel, F-34, Jet A-1 (source: fuels datasheet, [7])

	Fuel type		
Parameter	Diesel Fuel	F-34	Jet A-1
Density in 15ºC [kg/m^3]	831	804	796
Cetane number	50	45	42
Temp. ignition [ºC]	66	57	38
Viscosity at –20 ºC [mm^2/s]	2.210	3.102	3.815
Calorific value [MJ/kg]	43	42.35	42.28
CFPP [ºC]	–27	–54	–

2.2. The tested hybrid drive system

As mentioned in paragraph 1, LUMWP has a hybrid series combustion and electric drive system. Figures 4 and 5 show the actual location of the ICE and the generator on the vehicle.

Fig. 4. LUMWP without upper body and battery removed, isometric view

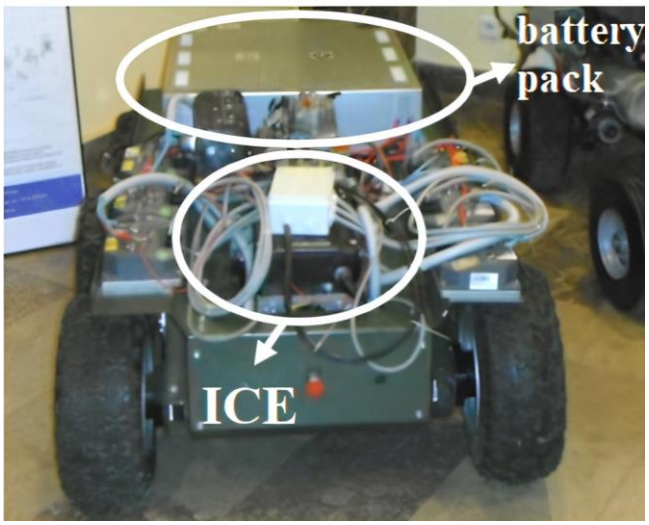

Fig. 5. LUMWP without upper body, front view

The tested hybrid drive system consists of a generating set: Yanmar L100AE diesel engine (technical information of the CI engine is shown in Table 2 below) and E1S10L KE synchronous generator (technical information of the generator is shown in Table 3 below), and a lithium-polymer electrochemical battery (technical information battery is shown in Table 3).

Table 2. Selected technical data of the Yanmar L100AE engine [source: user manual, 22]

Engine type	Yanmar L100AE
Construction	CI, air-cooled, single-cylinder
Power type	Direct injection, piston pump, mechanical injection
Stroke capacity	406 cm³
Bore x stroke	86×75 mm
Maximum power for the base fuel	6.5 kW
Crankshaft operating speed	~3000 rpm

The Yanmar L100AE engine was combined to work with a synchronous generator, the technical data of which are presented in Table 3 below.

Table 3. Technical data of the E1S10L KE generator (source: user manual, [22])

Generator type	E1S10L KE
Construction	Self-excited, synchronous
The type of electricity produced	AC, three-phase 50 Hz
Rated voltage	400 V
Rated power	7.0 kVA
Insulation class	H

The task of the generator is to charge the lithium-polymer $LiFePO_4$ battery. It consists of a stack of twelve lithium-polymer cells connected in series. Inside the battery housing is a compartment for electrical connectors, a rectifier unit, and a BMS (Battery Management System) which supervises the proper operation of all cells during battery charging and discharging [15]. This system prevents the battery from discharging to a level that could lead to irreversible damage, as well as monitors which of the battery cells is weak or damaged. The BMS system also measures cell and ambient temperatures. Inside the battery, there is a system protecting it against excessive load. Based on these data, the system assesses the condition of the cells, and in the event of a failure or overtemperature, it disconnects the battery from the output terminals. The battery is equipped with a diagnostic interface that allows to control the battery operation via a computer network. The battery parameters are presented in Table 4.

Table 4. Basic technical data of the tested lithium-polymer battery [source: user manual, provided by the battery manufacturer Wamtechnik, battery cells made by Kokam]

Rated capacity	70 Ah
Rated operating voltage	44.4 V (3.7 V/cell)
maximum charging current	70 A
Minimum discharge voltage	2.70 V/cell ±0.05 V = 32.4 V
Permissible operating temperature	–20–45°C (discharging)| 0–40°C (charging)|

The theoretical course of engine load related to charging (Fig. 6) furthermore, resulting from the operation of the generator and the battery BMS module distinguishes two stages:

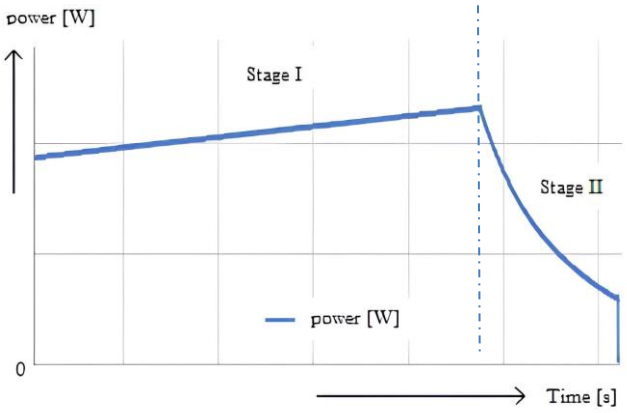

Fig. 6. Theoretical electrical loading diagram of the tested engine over time

– Stage I: the battery is charged with constant current until the appropriate cell voltage is obtained
– Stage II: BMS, after obtaining the appropriate cell voltage in the battery, maintains this voltage and reduces the current until the end of charging.

2.3. Description of the measuring station

The test stand set up to test the operational properties of the hybrid drive system powered by substitute fuels is shown in Fig. 7.

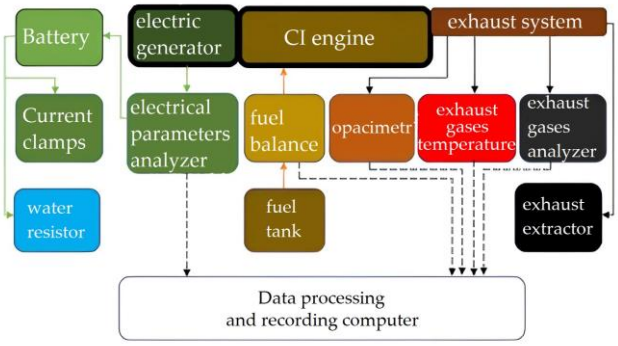

Fig. 7. Schematic layout of the research stand [author's source]

In order to analyze and record current data during the tests, the BMR trading PLA34 analyzer was used, with three voltage inputs and eight current inputs for measuring electrical parameters. The PLA34 works by continuously sampling the voltage and current inputs at 40 kHz. PLA34 is an instrument for monitoring power quality in accordance with the EN 50160 standard [5]. The analyzer was connected in series between the generator and the battery.

Fuel consumption during the tests was determined using the AVL 733S Fuel Balance fuel scale [3]. This device determines fuel consumption by means of a suitable weighing vessel connected to a bending beam with a capacitive displacement sensor. Due to the fact that the weighing vessel must be replenished for each measurement, this is

a discontinuous measurement principle. The mass of the fuel consumed is thus determined gravimetrically, which means that the density need not be additionally determined. Fuel consumption can be determined with an accuracy of 0.12%. The built-in calibration unit is standard equipment and allows calibration and accuracy control according to ISO 9001 [8]. The scale saves data in the form of hourly fuel consumption G_e [3].

Exhaust gas opacity was measured using the AVL 439 OPACIMETER, which operates on the principle of light absorption [2]. The AVL 439 opacimeter measures the transparency of polluted air, in particular exhaust emissions from diesel engines. The measuring chamber with a defined measuring length and non-reflecting surface is evenly filled with exhaust gases. The light intensity loss between the light source and the receiver is measured and the exhaust gas transparency is calculated from it. The calculations are based on the Lambert-Beer law [2, 6]. The opacimeter collects exhaust gas samples from the engine exhaust manifold, where the appropriate ½ inch threaded connection is mounted.

A set of exhaust gas analyzers CEB II – 2000 was used to analyze the shares of gaseous components of exhaust gases. It is a fully automated, computer-controlled set of measuring instruments. Exhaust gases collected using a probe mounted on the exhaust manifold were pre-filtered and then flowed through the gas path to the exhaust gas dosing unit for individual analyzers. Water vapor was condensed from the exhaust gases and directed to the "cold exhaust gas analyzers" in the cooler located in the measuring cabinet with analyzers. Exhaust gases for the analyzers requiring hot exhaust gases were supplied through a heated gas path. The CO and CO_2 analyzers operated by absorbing infrared radiation. All analyzer modules are built into the gas sample conditioning cabinet. Reference gases, two concentrations of each of the measured exhaust gas components, were supplied to the analyzers [1]. The gas cylinders were placed in a rack and connected to the analyzers with teflon hoses.

The exhaust gas temperature was measured using a thermocouple. The thermocouple consists of a pair of dissimilar metals, usually in the form of wires, bonded at both ends. The thermocouple used in the tests consisted of NiCr–NiAl. The operating range of this thermocouple is 50–400 ±1°C. The thermocouple was mounted in the exhaust manifold on which the appropriate M5 threaded connection was welded. Analog data from thermocouples were converted into digital form by a computer module.

HP-605A current clamps were used during the battery discharge. With their participation, the values of the discharge current flowing through the cable connecting the battery with the water resistor were monitored.

The water resistor is a device used in the tests to discharge the electric battery of the system. It is made of elements produced from stainless steel. The resistor converts electrical energy into work in the chemical process of water hydrolysis.

The fuel tank with a capacity of 5 dm^3 was placed above the fuel scale. The fuel from the tank to the fuel scale flowed by gravity.

The tests were carried out in a closed room. In order to maintain occupational health and safety, exhaust fumes were discharged into the atmosphere outside the building using an exhaust extractor powered by an electric motor.

The control of the test stand and the recording of measurement results were carried out using a series of computers equipped with appropriate measurement and control modules and appropriate software.

2.4. Method of conducting measurements of performance properties of the tested vehicle's propulsion

Exploitation is defined as a set of purposeful organizational, technical, and economic activities of people with equipment and mutual relations between them from the moment of accepting the equipment for use in accordance with its intended purpose until its liquidation [17, 24]. In the context of the tested hybrid vehicle, the measurement of operational properties consists of examining:

- times of full charge – telling, among others, about the speed of the ability to perform tasks by the tested unmanned vehicle (the shorter, the better)
- the amount of fuel used to fully charge – talking about, for example, the frequency of refueling (the less often, the better) or the cost of its operation (the smaller the better)
- the values of the exhaust gas components – showing the level of environmental performance during the use of this vehicle (the lower the CO and CO_2 content, the better).

In order to determine these properties, tests of the hybrid system were carried out for three selected fuels. The first stage of the research was to fill the tank with the fuel used in the test. When changing fuel to another engine fuel system (filter, fuel lines), the fuel scale and the tank were previously drained. The lithium-polymer battery was discharged using a water resistor. In order to maintain the repeatability of the tests, the battery was discharged with a DC current of ~50 A. The discharge current values were monitored using current clamps. By adjusting the depth of immersion of the resistor sheets in water, the value of the current flowing from the battery was determined. The BMS battery control system disconnects the discharge circuit automatically at the appropriate cell voltage level. After discharge, the battery remained idle for at least 30 minutes in order to "relax" the cells, i.e., restore their chemical and temperature stability. At that time, the diesel engine was started in order to warm it up to the operating temperature and possibly burn out the fuel residues from the previous test.

The next stage was the preparation of the analyzers: switching on the analyzer of electrical parameters, filling the fuel scale, and calibration of the exhaust gas analyzer. When all the measuring devices were ready for work, the engine was started and the battery charging process began.

The methodology of comparing the impact of selected substitute fuels on the tested hybrid system inform about determining the load characteristics of the internal combustion engine over time. The load characteristic of the engine is the dependence of the hourly fuel consumption as a function of power. This characteristic is used to evaluate motors that are characterized by a constant rotational speed. The

rotational speed of the shaft for the tested L100AE engine recommended by the manufacturer for the Diesel base fuel is 3000 rpm. Ideally, this value was set before the tests during engine operation on the base fuel. The load characteristics of the compression-ignition engine are determined during operational adjustment of the injection advance angle. The size of the dose of fuel injected into the engine is obtained by changing the position of the dose control element (i.e. the rack of the injection pump piston). At a fixed engine speed, the amount of air entering the cylinders is constant. The composition of the fuel-air mixture produced in the engine cylinders is, therefore variable. Therefore, the coefficient of excess air λ is also variable. As the amount of fuel injected increases, the combustion conditions change.

The element loading the diesel engine in the test was the generator, whose task was to carry out a full battery charging cycle. The element recording the value and change of the load over time was the analyzer of electrical parameters, which processed the measurements and calculations of all parameters and electrical values of the battery charging in real time before the battery rectifier system. Instantaneous fuel consumption values during the test were recorded by a fuel scale. Instantaneous flue gas composition values were recorded by the flue gas analyzer. The BMS disconnected the charging circuit automatically at the appropriate cell voltage level. The end of charging was a sign to turn off the internal combustion engine and end the research. The battery, as in the case of discharging after charging, remained idle for at least 30 minutes in order to "relaxation". All tests were carried out in a closed room at 20°C.

All results of parameter measurements were observed and collected throughout the experiment and during the tests for the purpose of ongoing control of the technical condition of the hybrid system and measuring instruments, and determination of the circumstances of a possible failure, and control of the implementation of subsequent phases of the research cycle. The measurement results downloaded from the analyzers were processed on a computer using the Microsoft Excel program and presented on charts.

2.5. Mathematics formulas used to develop measurement results [17]

Below are the mathematical formulas used to develop the test results:

– charging active power P_t at time t [W]:

$$P_t = (I_1 \cdot U_1 \cdot \cos\varphi_1)_t + (I_2 \cdot U_2 \cdot \cos\varphi_2)_t + (I_3 \cdot U_3 \cdot \cos\varphi_3)_t \quad (1)$$

where: I_1 – phase current 1 [A], I_2 – phase current 2 [A], I_3 – phase current 3 [A], U_1 – phase voltage 1 [V], U_2 – phase voltage 2 [V], U_3 – phase voltage 3 [V], φ_1 – phase shift angle 1 [rad], φ_2 – phase shift angle 2 [rad], φ_3 – phase shift angle 3 [rad]

– total active charging energy E_l [W·h]:

$$E_l = \sum_t^n (P_t \cdot t) \quad (2)$$

– charging reactive power Q_t at time t [var]:

$$Q_t = (I_1 \cdot U_1 \cdot \sin\varphi_1)_t + (I_2 \cdot U_2 \cdot \sin\varphi_2)_t + (I_3 \cdot U_3 \cdot \sin\varphi_3)_t \quad (3)$$

where: I_1 – phase current 1 [A], I_2 – phase current 2 [A], I_3 – phase current 3 [A], U_1 – phase voltage 1 [V], U_2 – phase voltage 2 [V], U_3 – phase voltage 3 [V], φ_1 – phase shift angle 1 [rad], φ_2 – phase shift angle 2 [rad], φ_3 – phase shift angle 3 [rad]

– mass fuel consumption [kg]:

$$\sum_t^n (G_e \cdot t) = \text{mass fuel consumption} \quad (4)$$

where: G_e – fuel consumption [kg/h], t – time [h].

– energy produced [MJ]

$$\text{energy produced} = \frac{E_l}{1000000 \cdot 3600} \quad (5)$$

– energetic efficiency [%]:

$$\text{energetic efficiency} = \frac{\frac{\text{energy produced}}{\text{calorific value}}}{\text{mass fuel consumption}} \cdot 100\% \quad (6)$$

3. Results

This section will discuss the external charging characteristics for 3 types of fuels, common statements regarding hourly fuel consumption, Active charging power, Reactive power, and emission lists of selected exhaust gas components (including temperature and smoke). Mass fuel consumption, energy produced and overall energy efficiency are also presented.

3.1. Charging load characteristics and exhaust emission for Diesel fuel

Figure 8 below shows the characteristics of the load as a function of time performed on the diesel base fuel. The battery charging system forced a current-voltage waveform that loaded the diesel engine. The power curve of the internal combustion engine is marked in blue. The hourly fuel consumption changed analogously to the course of the power generated by the diesel engine. A full charging cycle lasted 1:29:34 hours, and 1.14 kg of diesel fuel was used to charge the battery.

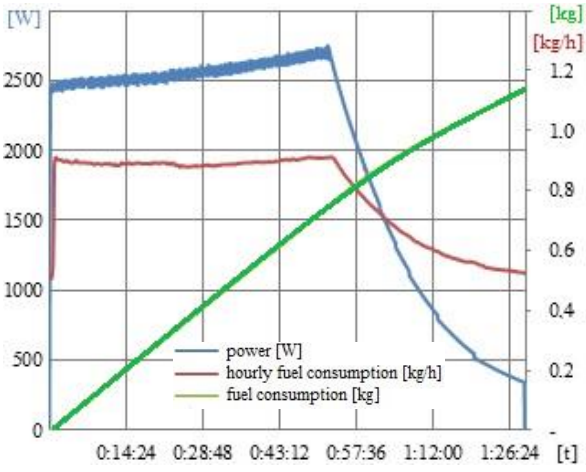

Fig. 8. Load characteristics as a function of time for diesel fuel

In Figure 9 presents the course of the percentage share of selected exhaust gas components during the performance of the load characteristics on the base fuel (diesel). The runs of the exhaust gas components change analogously to changes in the diesel engine load.

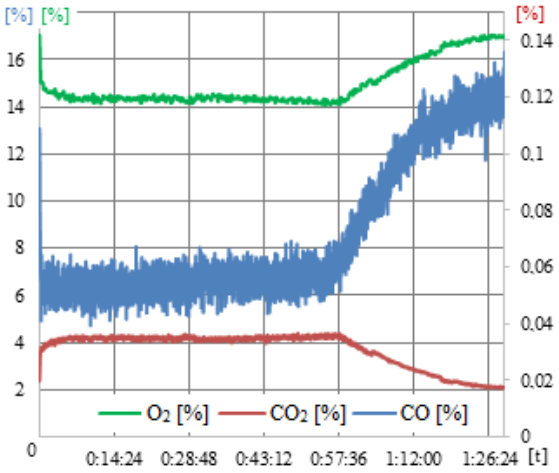

Fig. 9. Percentage share of selected exhaust gas components for diesel fuel

3.2. Charging load characteristics and exhaust emission for F-34

Figure 10 presents the load characteristics of a diesel engine made on the F-34 substitute fuel for a diesel engine being part of a serial hybrid propulsion system of an unmanned platform. During the test, the internal combustion engine maintained the rotational speed of the engine shaft at ~2850 rpm without changing the settings of the speed controller. A full charging cycle lasted 1:49:26 hour, and 1.46 kg of F-34 fuel was used to charge the battery.

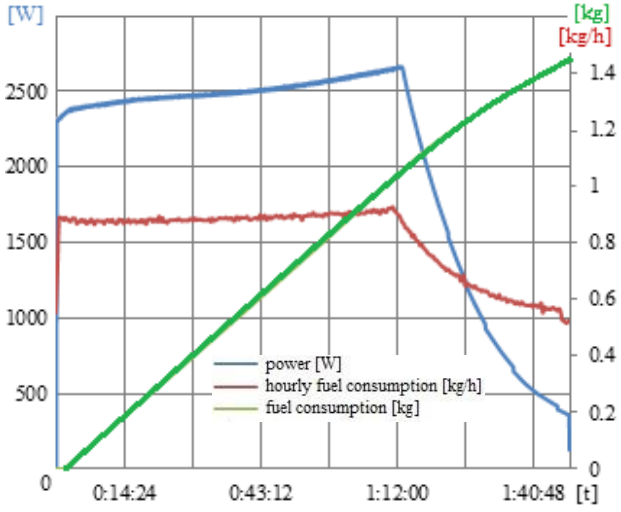

Fig. 10. Load characteristics as a function of time performed on substitute fuel F-34

Figure 11 presents the course of the percentage share of selected exhaust gas components during the performance of the load characteristics on the substitute F-34 fuel. The runs of the exhaust gas components change analogously to changes in the diesel engine load.

3.3. Charging load characteristics and exhaust emission for Jet A-1

Figure 12 shows the time load characteristics of a compression-ignition engine (part of a series hybrid drive system) made on substitute fuel, a mixture of Jet A-1 fuel. During the test, the internal combustion engine maintained the rotational speed of the engine shaft at ~2830 rpm without changing the settings of the speed controller. A full charging cycle lasted 1:52:52 hours, and 1.61 kg of Jet A-1 was used to charge the battery.

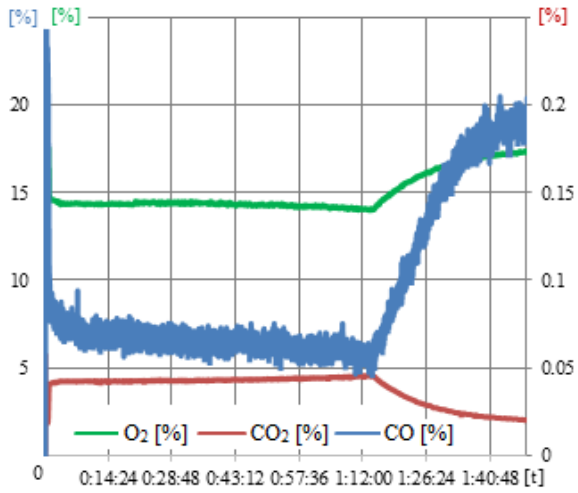

Fig. 11. Percentage of selected exhaust gas components for F-34 fuel

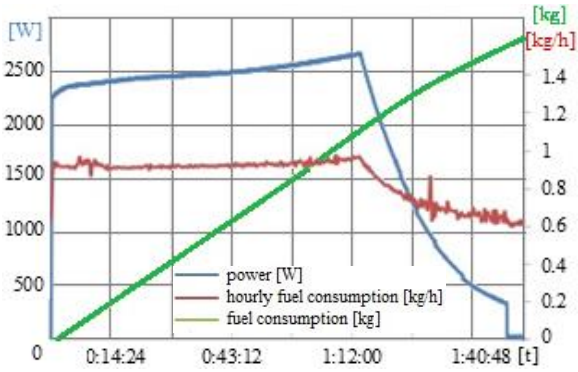

Fig. 12. Load characteristics over time performed Jet A-1

Figure 13 shows the course of the percentage share of selected exhaust gas components during the performance of the load characteristics on the substitute fuel – Jet A-1 fuel mixing. The runs of the exhaust gas components change analogously to changes in the diesel engine load.

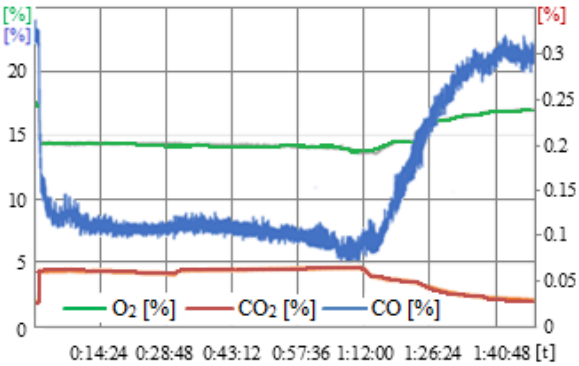

Fig. 13. Percentage of selected exhaust gas components for F-34 fuel

3.4. Common results for all tested fuels

3.4.1. Hourly fuel consumption

Due to the differences in the calorific values of fuels and the decrease in the charging power resulting from the

change in engine speed on the substitute fuels, the hourly fuel consumption values differ, as shown in Fig. 14.

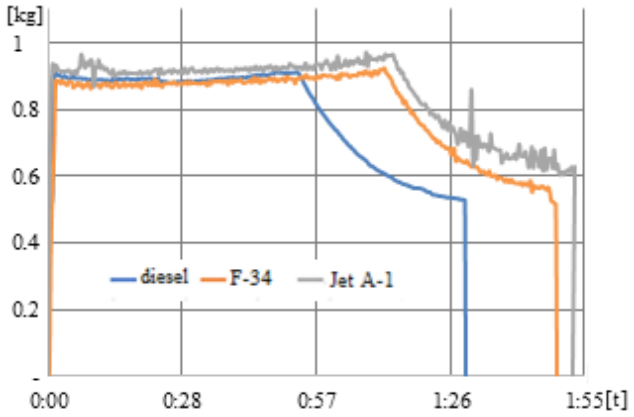

Fig. 14. Summary of hourly fuel consumption over time for diesel, F-34 and Jet A-1

3.4.2. Active charging power

Figure 15 shows the active power generated during the tests for individual fuels. Active power is the part of the power that the load takes from the source and converts it to work or heat. The differences in the power generated for the base and substitute fuels result from the difference in the rotational speed of the engine crankshaft and thus, the generator rotor. This affects the desynchronization of the generator's operation and the increase in reactive power generation. The difference between the tested substitute fuels results from the difference in calorific value

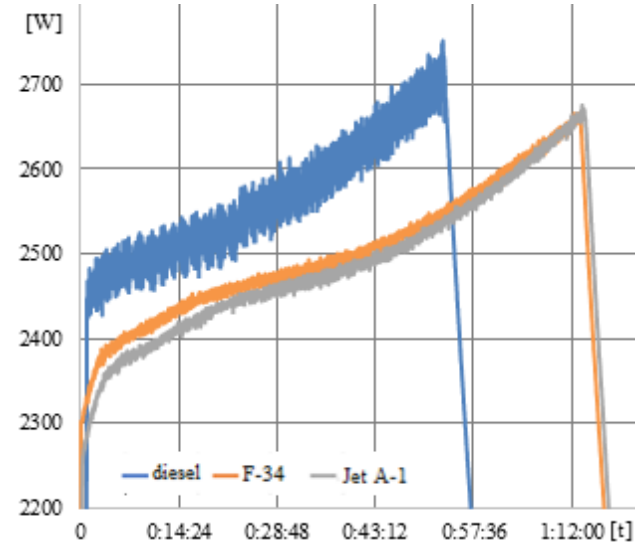

Fig. 15. List of active power over time for diesel, F-34 and Jet A-1

3.4.3. Reactive power

Reactive power in AC circuits is a quantity describing the pulsation of electric energy between the elements of the electric circuit. This oscillating energy is not converted into useful work or heat, but it is necessary for the generator to function in the hybrid system under investigation. Differences in generated reactive power have a direct impact on active power [8]. Figure 16 shows the reactive power generated during the tests for individual fuels.

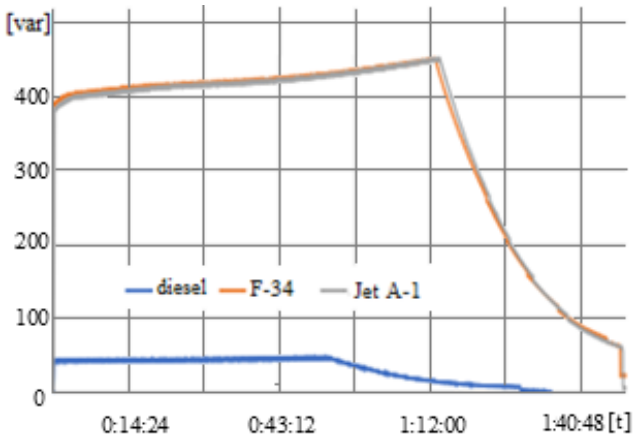

Fig. 16. Summary of reactive power over time for diesel, F-34 and Jet A-1

3.4.4. Exhaust gases composition

Carbon dioxide

Figure 17 presents the percentage share of carbon dioxide in exhaust gases for the base and tested substitute fuels. The graph shows that the carbon dioxide values oscillate in similar values for each of the tested fuels. Slightly higher contents for substitute fuels result from their incomplete combustion.

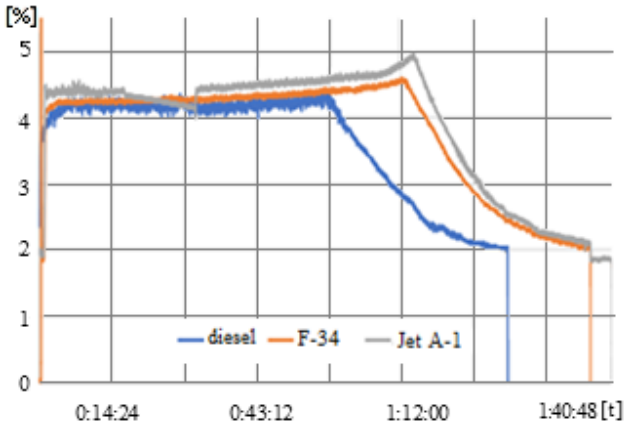

Fig. 17. A summary of the percentage of carbon dioxide in the exhaust gas composition over time for diesel, F-34 and Jet A-1

Oxygen

Figure 18 shows the percentage share of oxygen in the exhaust gas for the base fuel and the tested substitute fuels. The graph shows that the oxygen values in the exhaust gases are similar. Similar amounts of oxygen particles contained in the tested fuels are also reflected in the exhaust gas composition.

Carbon monoxide

Figure 19 presents the percentage share of carbon monoxide in exhaust gases for the base fuel and the tested substitute fuels. The chart shows that Jet A-1, due to less effective combustion (e.g. lower exhaust gas temperature) and the content of additional carbon particles in the admixture, is characterized by the highest content of carbon monoxide in exhaust gases [9].

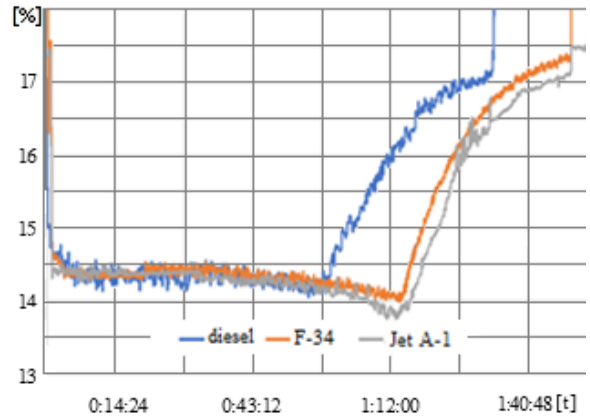

Fig. 18. Summary of the percentage of oxygen in the exhaust gas composition over time for diesel, F-34 and Jet A-1

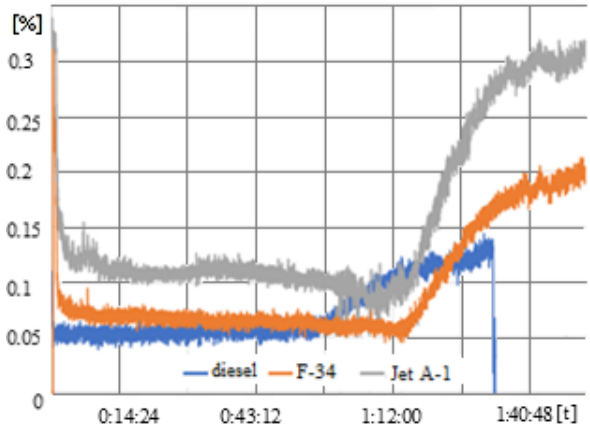

Fig. 19. Percentage of carbon dioxide in the composition of exhaust gases over time for diesel, F-34 and Jet A-1

Exhaust smoke opacity

Figure 20 presents smoke opacity for the base fuel and the tested substitute fuels. The graph shows that smoke opacity for substitute fuels is higher by about 30% throughout the charging process.

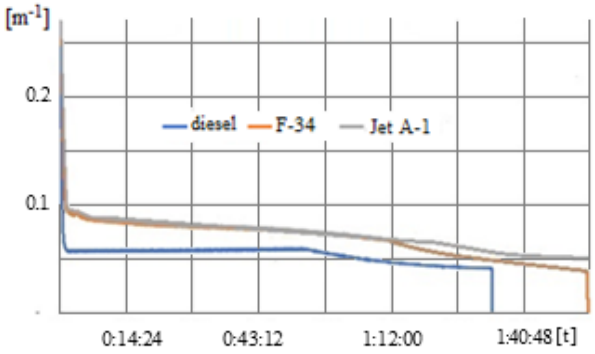

Fig. 20. Comparison of smoke opacity over time for diesel, F-34 and Jet A-1

Exhaust gases temperature

The exhaust gas temperature (Fig. 21) during the test was the highest for diesel fuel. This indicates the most efficient combustion. The exhaust temperature of the F-34 fuel is higher than that of Jet A-1, most likely due to the higher calorific value.

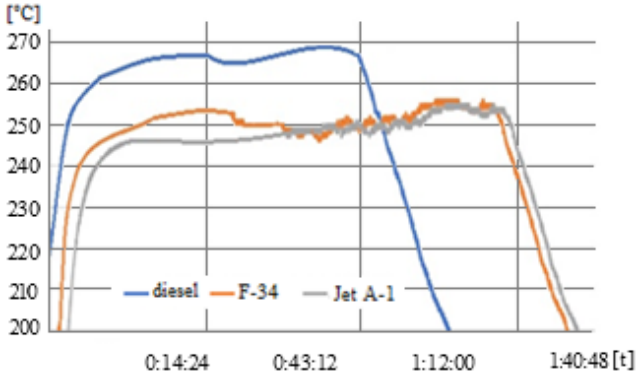

Fig. 21. Comparison of exhaust gas temperature over time for diesel, F-34 and Jet A-1

3.4.5. Mass fuel consumption

Figure 22 presents the total mass amount of fuel needed for a full charging cycle of the battery of the tested system.

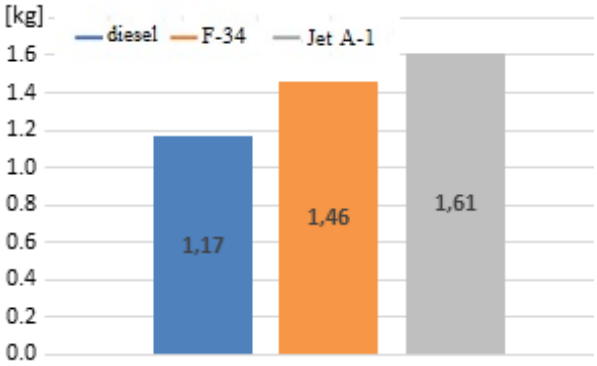

Fig. 22. Mass fuel consumption per charging cycle for diesel, F-34 and Jet A-1

3.4.6. Energy produced

Figure 23 summarizes the total amount of electricity needed to fully charge the battery during the tests for individual fuels. Different charging powers most likely affected the temporary current-voltage state of the battery cells, and thus the reaction of the BMS. Therefore, the battery charging control system disconnected the charging circuit at different values of energy produced by the generator.

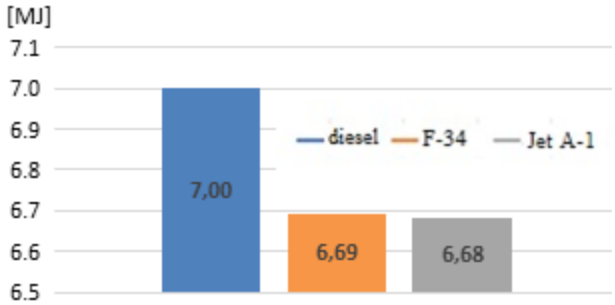

Fig. 23. Total energy produced from diesel fuel, F-34 and Jet A-1

3.4.7. Energetic efficiency

Figure 24 shows the overall efficiency of converting the energy contained in the fuel into electricity for individual fuels.

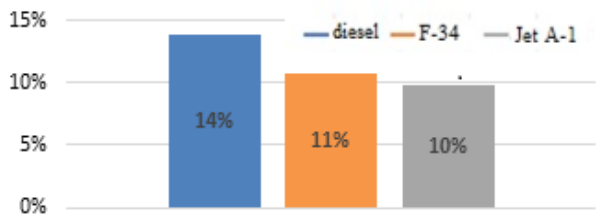

Fig. 24. Total engine energy efficiency using diesel, F-34 and Jet A-1

4. Discussion

In the tested hybrid drive system, the transition to the substitute fuels used in the test, due to the fact that the chemical composition is very similar to the base fuel, can take place at any time. The tested combustion engine can successfully use them without structural changes and fully charge the battery.

The construction of the injection system and the speed controller in the tested internal combustion engine as well as large differences in the viscosity and calorific value of the tested substitute fuels resulted in a 5–6% decrease in the rotational speed of the engine shaft. The engine speed maintenance system is not fully adapted to the use of other fuels. The rotational speeds of the generating set-in series hybrid systems are most often selected in a way that guarantees their most effective operation. The internal combustion engine operates at the point of the lowest specific combustion, and the generator at the point where the losses resulting from the generated reactive power are compensated or minimized. Changing the rotational speed has negative consequences in the form of a decrease in the energy efficiency of the entire system [15]. In terms of operational properties, this results in increased charging time (22% for F-34 and 26% for Jet A-1), increased fuel consumption (26% for F-34 and 41% for Jet A-1) and more frequent refueling. However, in ad-hoc situations, tested alternative fuels can be used. Changing the volumetric size of the injected fuel (moving the injector's control rack, or using a different speed regulator system) to a larger one would increase the efficiency of the generator. At the same time, the entire system, and recommended changing it in long-term applications of the tested substitute fuels. Literature analysis indicates that with long-term use due to the low viscosity and very good cleaning properties of the tested alternative fuels, any faults in the fuel system may be revealed [6, 12, 14]. This may exacerbate the decline in energy efficiency. Also, the lower cetane number of the tested alternative fuels may impair the cold start of the engine and increase the tendency to hard work. Due to the lower combustion temperature of substitute fuels, a greater amount of incomplete combustion products and greater opacity of exhaust gases can be observed in the exhaust gases. Both this and the very fact of the longer charging process indicate the negative effects of the use of the tested substitute fuels in the ecological context. In the propulsion system, the transition to the substitute fuels used in the test, due to the fact that the chemical composition is very similar to the base fuel, may take place at any time. The tested combustion engine can successfully use them without structural changes and fully charge the battery.

5. Summary and final conclusions

The modern development of hybrid drive systems takes into account the need to combine conflicting requirements. On the one hand, ecological requirements are growing, on the other hand, these systems are required to obtain maximum work units. The continuous development of hybrid systems increases the complexity of their construction. The internal combustion engines themselves also use very precise power and control systems to increase thermal efficiency. Precision fuel systems are very sensitive to changes in fuel parameters or contamination. Modern multi-element hybrid systems, in which various forms of energy are transformed several times, are therefore very susceptible to the influence of fuel on the quality of their work. Therefore, the use of alternative fuels in such systems should be part of the design process. The use of substitute fuels at this point may turn out to be very beneficial in the ecological context, and in the long term, their use due to the depletion of oil resources will be a necessity. The final conclusions are presented below:

– alternative fuels can be successfully used in internal combustion engines of hybrid drive
– in the tested serial hybrid propulsion system of the unmanned platform, it is possible to use F-34 fuel and Jet A-1 fuel
– if the above-mentioned fuels are used to propel the platform, one should be aware of the increased fuel consumption and the potential decrease in energy efficiency and the negative impact on the environment associated with increased exhaust emissions
– if there is an intention or need to use substitute fuels in modern multi-element hybrid systems, the possibility of using such fuels should be taken into account in the process of designing and constructing these hybrid systems. Thanks to this, they will maintain their high work efficiency.

Acknowledgements

This work was financed by Military University of Technology under research project UGB 22-833/2023.

Nomenclature

AC	alternate current
Al	aluminium
BLDCM	brushless direct current motor
BMS	battery management system
Cd	cadmium
CFPP	cold filter plugging point
CI	compression ignition
CO	carbon oxide
CO_2	carbon dioxide
DC	direct current
EN	European Standard
E_t	total active charging energy

F-34	NATO general use fuel
G_e	hourly fuel consumption
I	phase current
ICE	internal combustion engine
ISO	International Organization for Standardization
Jet A-1	type of aviation fuel
LUMWP	light unmanned military wheeled platform
NATO	North Atlantic Treaty Organization
Ni	nickel
O	oxygen
PC	personal computer
P_t	charging active power
Q_t	charging reactive power
t	time
U	voltage (phase voltage)
VAR	volt ampere reactive
λ	excess air factor
φ	current phase shift angle

Bibliography

[1] AVL CEB II – 2000 analyzer user manual.

[2] AVL. 439 Opacimeter product description. https://www.avl.com/documents/10138/885965/Download_01_AVL_439_Opacimeter_Product+Description.pdf (accessed on 27 April 2023).

[3] AVL. Product description: fuel balance. https://www.avl.com/documents/10138/2699442/Product+Description+Fuel+Balance (accessed on 22 April 2023).

[4] Barta D, Mruzek M, Kendra M, Kordos P, Krzywonos L. Using of non-conventional fuels in hybrid vehicle drives. Adv Sci Technol Res J. 2016;10:240-247. https://doi.org/10.12913/22998624/65108

[5] Elektroinstalator.com.pl. Jakość energii elektrycznej według normy PN-EN 50160. http://www.elektroinstalator.com.pl/index.php/artykuly/metrologia/2478-jakosc-energii-elektrycznej-wedlug-normy-pn-en-50160 (accessed on 24 April 2023).

[6] Heywood JB. Internal combustion engine fundamentals (2nd ed). McGraw-Hill Education 2018.

[7] Fuel data sheets obtained from the dealer – Regulation (EU) 2020/878 amending Annex II to the REACH Regulation.

[8] ISO 9001 – Quality management. https://www.iso.org/iso-9001-quality-management.html (accessed on 24 April 2023).

[9] Karczewski M, Szczęch L, Trawiński G. Motor vehicle engines (in Polish: Silniki pojazdów samochodowych). WSiP. Warsaw 2022.

[10] Kovbasenko S. Possibilities of enhancing the environmental safety of diesel vehicles using alternative fuels. J Mech Eng Transport. 2023;16:51-57. https://doi.org/10.31649/2413-4503-2022-16-2-51-57

[11] Khandelwal B. Aviation fuels (1st ed). Academic Press 2021.

[12] Legutko S. Machine operation (in Polish: Eksploatacja maszyn). Poznan University of Technology Publishing House. Poznań 2007.

[13] McDonnell K. Combat and tactical vehicles: developments and considerations for the department of defense. Military and Veteran Issues, 2nd ed. Nova Science Publishers, Inc. 2020.

[14] Merkisz J, Pielecha J. Alternative fuels and vehicle propulsion systems (in Polish: Alternatywne paliwa i układy napędowe pojazdów). Poznan University of Technology Publishing House. Poznań 2014.

[15] Merkisz J, Pielecha J. Electrical systems of hybrid vehicles (in Polish: Układy elektryczne pojazdów hybrydowych). Poznan University of Technology Publishing House. Poznań 2015.

[16] Nasoulis C, Protopapadakis G, Ntouvelos E, Gkoutzamanis V, Kalfas A. Environmental and techno-economic evaluation for hybrid-electric propulsion architectures. The Aeronautical Journal. 2023;127(1317):1904-1926. https://doi.org/10.1017/aer.2023.27

[17] National Radio Institute. Mathematics for Electronics and Electricity. 2017. USA.

[18] NATO. Logistic support agreement. https://www.nato.int/docu/logien/1997/lo-15a.htm (accessed on 24 April 2023).

[19] Schobert HH. The chemistry of hydrocarbon fuels (2nd ed.). Butterworth-Heinemann 2015.

[20] Shariz M, Gautam A, Tomar B, Gautam M, Jalil M. To Design an Optimal PV/diesel/battery hybrid energy system for Havelock Island in India. In: Rani A, Kumar B, Shrivastava V, Bansal RC (eds). Signals, machines and automation. International Conference on Signals, Machines, and Automation, Part of the Lecture Notes in Electrical Engineering book series (LNEE, 1023); 2023. https://doi.org/10.1007/978-981-99-0969-8_21

[21] Tanwar M, Tanwar P, Bhand Y, Bhand S, Jadhav K, Bhand S. Biofuels: production and properties as substitute fuels. IntechOpen 2023. https://doi.org/10.5772/intechopen.109073

[22] Yanmar. Silniki chłodzone powietrzem. https://yanmar.pl/silniki-yanmar/silniki-chlodzone-powietrzem/dsh$sajn2 (accessed on 24 April 2023).

[23] Zou Y, Li J, Hu X, Chamaillard Y. Modeling and control of hybrid propulsion system for ground vehicles. Springer Berlin, Heidelberg 2018. https://doi.org/10.1007/978-3-662-53673-5

Janusz Chojnowski, MEng. – Faculty of Mechanical Engineering, Military University of Technology in Warsaw, Poland.
e-mail: *janusz.chojnowski@wat.edu.pl*